J. Fluid Mech. (1993), *vol.* 248, *pp.* 543–566

The interaction between a steady jet flow and a supersonic blade tip

By N. PEAKE

Department of Applied Mathematics and Theoretical Physics, University of Cambridge, Silver Street, Cambridge, CB3 9EW, UK

(Received 14 July 1992 and in revised form 24 October 1992)

The potentially high level of noise generated by modern counter-rotation propellers has attracted considerable interest and concern, and one of the most potent mechanisms involved is the unsteady interaction between the tip vortex shed from the tips of the forward blade row and the rear row. In this paper a model problem is considered, in which the tip vortex is represented by a jet of constant axial velocity, which is convected at right angles to itself by a uniform supersonic mean flow, and which is cut by a rigid airfoil with its chord aligned along the mean flow direction. Ffowcs Williams & Guo have previously considered this problem for an infinite-span airfoil and a circular jet; in this paper we extend their analysis to include the effects of the presence of the second-row blade tip on the interaction, by considering a semi-infinite-span airfoil. As a first attempt, the case of a highly compact jet, represented by a delta-function upwash on the airfoil, is considered, and both the total lift on the airfoil and the radiation are investigated. The presence of the airfoil corner and side edge is seen to cause the lift to decay in time from its infinite-span value towards zero, due to a spanwise motion round the side edge; whilst the radiation is shown to be composed of two signals, the first received directly from the interaction between the jet and the leading edge, and the second resulting from the diffraction of sound waves emanating from the leading edge by the side edge. The effect of choosing a more diffuse upwash distribution is then considered, in which case it becomes clear that the first signal has a considerably larger amplitude, and shorter duration, than the second, diffracted signal.

1. Introduction

The interaction between the tip vortex shed by the forward row and the counter-rotating rear row is a powerful mechanism of sound generation in modern propeller systems. An accurate calculation of this noise must involve a number of demanding steps, and must at least include a realistic prediction of the source structure (that is, of the vorticity shed by the front row), a prediction of the noise generation resulting from the interaction of the rear row with this vorticity, and some consideration of the complicated propagation of the sound through inhomogeneities in the flow and round the other blades. Such a computation would clearly represent a very considerable undertaking, and given the present limited understanding of the whole process does not seem possible; for instance, whilst experiments on the structure of the tip vortex have been reported by Vaczy & McCormick (1987) and Simonich, McCormick & Lavich (1989), little quantitative information is as yet available on the tip vortex structure. The solution of simple model problems relevant to these three processes is

clearly critical, therefore, both as a means of understanding the physics, and in order to provide some estimate of the relative importance of the various mechanisms.

In this paper we shall only be concerned with the sound generation process, and shall therefore consider the unsteady interaction between what we believe is a reasonable, highly simplified, representation of the tip vortex and a model blade, and suppose that the resulting radiation propagates through uniform flow. We shall also be neglecting the blade rotation in determining this unsteady response, by supposing that the rear row blade is moving in a straight line at the appropriate local helical velocity, which will presumably be a reasonable assumption when calculating quantities evaluated in the neighbourhood of the blade surface, such as the blade loading, since the blade would in practice rotate by only a negligible amount during its very rapid interaction with the tip vortex. On the other hand, this rectilinear representation will clearly not provide a sensible estimate of the noise, since the radiation produced by sources in rectilinear motion is very different from that produced by rotating sources. However, an understanding of the radiation in our simplified rectilinear problem is still important as a first step, since it does provide an indication of acoustical energy levels being projected to the far field, and, as will be seen, provides some understanding of the various mechanisms. We shall represent the tip vortex core by a jet whose axial velocity is constant in time and whose transverse extent is relatively small, and which is cut at right angles by the blade. This seems a particularly attractive model for the tip vortex, since it both proves amenable to analysis and contains the most significant feature of the real flow, namely that the tip vortex will be tightly rolled up for the high, possibly supersonic, tip speeds envisaged for modern propellers.

A considerable amount of attention has been devoted to such problems concerning the interaction between some known disturbance and an airfoil; for instance, Amiet (1976, 1986*a*), who considers the interaction between a harmonic gust and an infinite-span airfoil in uniform subsonic flow. With particular relevance to the question of tip-vortex noise, Ffowcs Williams & Guo (1988) and Guo (1990) considered the interaction of a circular uniform-axial-velocity jet with an infinite-span, supersonic airfoil (Amiet 1986*b* solved the subsonic version of this problem). In these jet problems, noise is generated when the leading edge of the airfoil intersects the jet, forcing a sudden readjustment in the near-field flow round the airfoil in order to satisfy the normal velocity boundary condition. This noise is particularly intense, and in the supersonic problem Ffowcs Williams & Guo (1988) even predicted that along a single 'Mach wave' direction in the jet rest frame these acoustic waves propagate to the far field unattenuated, with an amplitude of typically 160 dB or more. Such an effect can clearly not occur in the subsonic case, but even then an intense, large-amplitude signal was predicted by Amiet (1986*b*), at least for a relatively compact jet. As well as the initial signal resulting from the leading-edge interaction, a secondary weaker and less intense signal was predicted for both subsonic and supersonic problems, arising from the diffraction of sound generated at the airfoil leading edge by the trailing edge (for the supersonic case see in particular Guo 1990). Consideration of these simple jet–airfoil interaction problems has therefore confirmed that the interaction between the tip vortex and a blade is capable of producing considerable, subjectively annoying, noise levels, and in this paper we seek to include one further feature, namely the presence of the blade tip. Since the blade lengths in the front and rear rows of modern propellers are likely to be equal, it is clear that the front-row tip vortex will interact with the rear-row blade near the blade tip, and the question of the effect of the blade tip on the noise is

therefore an important one, which has not been addressed by the analysis of infinite-span airfoils mentioned above. We also note that real propeller blades are swept, so that the leading edges are no longer at right angles, but this will not be considered here.

We shall restrict attention to the case of supersonic motion, and as a first step in the analysis we shall suppose that the rear-row blade is unswept and is rectangular (i.e. untapered) at the tip. Further, since the effects of the trailing edge have been considered in detail by Guo (1990), we shall neglect its presence here, and represent the blade by a rigid quarter-plane (i.e. an airfoil which is semi-infinite in two perpendicular directions). Supersonic flow past a quarter-plane has previously been studied by Stewartson (1950) and Miles (1951), who both considered the related problem of the unsteady lift distribution on a fluttering quarter-plane, whilst more recently Martinez & Widnall (1983) and Peake (1992) have considered harmonic gust–corner interaction in subsonic and transonic flow respectively. As has already been stated, however, our aim here is to study the effects of a jet-like upwash, as motivated by Ffowcs Williams & Guo's approach (side-edge effects in airfoil–vortex interaction have already been considered by Howe 1989 in the case of a circular airflow in low Mach number flow). As a starting point for our analysis, and as a means of providing a simple description of the radiation mechanisms, we consider a highly compact jet, which we shall represent by a delta-function normal velocity distribution on the quarter-plane, as is done by Amiet (1986*b*), and once this has been completed we repeat the analysis for a more diffuse upwash, in which the jet velocity possesses a Gaussian distribution (again in parallel to Amiet 1986*b*). We shall work in the aerodynamic frame, in which the quarter-plane is at rest, and the jet is convected by the supersonic mean flow.

The paper is divided into sections, as follows. In §2 we describe the mathematical formulation, and the formal solution of the problem for the delta-function jet, which is completed using complex variable methods and the Wiener–Hopf technique. In §3 we consider the total lift on the quarter-plane, and an analytic expression for the variation of the lift with time is found. Before the jet intersects the quarter-plane, the lift is of course zero, but once the interaction has occurred we shall see that there is a time interval in which disturbances from the leading-edge–jet interaction have not yet propagated to the side edge, so that the lift takes the value that it would have done in the infinite-span case; once acoustic waves generated by the leading-edge–jet interaction have reached the side edge, however, a spanwise motion around the side edge, from pressure surface to suction surface, is set up, which acts to reduce the total lift towards zero.

In §4 we consider the radiation in the delta-function jet case. We see that sound is received by observers positioned on and inside a cone with its apex at the quarter-plane corner and with semi-vertical angle $\sin^{-1} 1/M$, and expressions for the acoustic pressure, valid strictly inside this cone, are derived. The radiation is seen to be composed of two distinct signals (which are singularities in this case, due to our choice of a singular upwash); the first signal (here a delta function), is a result of the jet–leading-edge interaction alone, and is exactly equal to the infinite-span result of Guo (1990); whilst the second signal (here an inverse square root singularity) results from the diffraction of the leading-edge sound by the side edge. We prove in an Appendix that the arrival time of this second signal corresponds exactly to the shortest time taken by acoustic waves to travel from the point of intersection of the jet with the leading edge to the side edge, be diffracted by the side edge, and then reach the observer in the far field.

Of course, whilst our use of a delta-function upwash has simplified the analysis, and indicated how the various components of the radiation are generated, such a singularity is physically unrealistic, and in §5 we therefore repeat the radiation calculation for a more diffuse (Gaussian) upwash distribution; we shall, however, suppose that the characteristic length of this Gaussian is small. The resulting radiation field is just a smoothed-out, non-singular version of the delta-function result, and again contains two signals, generated by the interaction of the jet with the leading edge and the diffraction of the leading-edge sound by the side edge respectively. However, it is now possible to compare the relative intensities and durations of the two signals, and it becomes clear that the second (diffracted) signal has a significantly smaller amplitude and longer duration than the first signal. The structure of the radiation, consisting of a large impulsive pressure peak, followed by a second, less intense signal of the opposite sign, is in fact very similar to that found for the interruption of a jet by an infinite-span, but finite-chord, airfoil by Guo (1990) in supersonic flow and Amiet (1986*b*) in subsonic flow.

As we have already mentioned, the question of the intense, unattenuated, pulse of radiation which is transmitted along the critical Mach-wave direction in the jet rest frame has already been considered by Ffowcs Williams & Guo (1988) for the infinite-span airfoil, and such a pulse, resulting from the initial interaction between the jet and the leading edge, would clearly also be present in our quarter-plane problem (we note that the Mach-wave direction in the jet rest frame corresponds to a single direction lying on the cone with apex at the corner and semi-vertical angle $\sin^{-1} 1/M$ in our blade-fixed frame). This pulse would be unaffected by the presence of the corner, however, since no diffracted sound from the side edge could subsequently catch up with it, and its magnitude is probably best predicted using the (infinite-span airfoil) techniques described by Ffowcs Williams & Guo (1988); this single, Mach-wave, observer direction will therefore not be considered here. In all other observer directions, we shall see that the radiation decays with observer distance due to spherical spreading.

2. Mathematical formulation

We consider a rigid quarter-plane occupying the quadrant $\{x > 0, y > 0\}$ of the plane $z = 0$, surrounded by a uniform supersonic mean flow of speed U parallel to the x-axis; the semi-infinite leading and side edges of the quarter-plane are therefore aligned along the y- and x-axes respectively. Since modern propeller blades are thin, we shall suppose as a first approximation that the quarter-plane possesses zero thickness. A jet, with its axis aligned parallel to the z-axis and with its axial velocity constant in time, is convected by the mean flow, and is incident on the quarter-plane from upstream; in the first instance we suppose that the jet axial velocity distribution is highly compact and can be represented by a delta function, so that the upwash velocity on the quarter plane is of the form

$$V\delta(x-Ut)\,\delta(y-y_0)\,\mathbf{z}, \tag{1}$$

where $\mathbf{z}$ is the unit vector parallel to the z-axis. Here, V is the volume flux of the jet across the plane $z = 0$, and y_0 (which is positive) corresponds to the perpendicular distance between the corner and the path of the jet; the system is shown in figure 1. We see that the jet intersects the leading edge of the quarter-plane at the instant $t = 0$. The convention adopted here for the direction of the jet velocity is opposite to that used by Ffowcs Williams & Guo (1988) and Guo (1990).

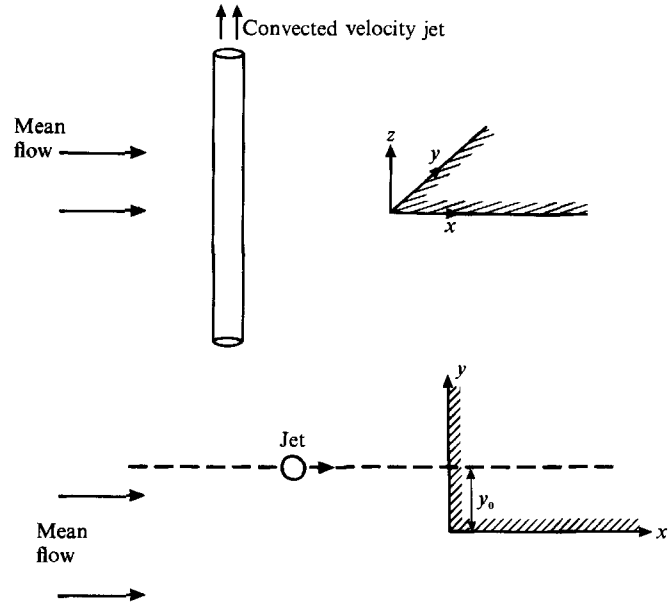

FIGURE 1. The geometry of the problem; (*a*) perspective view; (*b*) plan view.

The interaction between the jet and the rigid quarter-plane will induce a perturbation velocity, $\boldsymbol{u}$, and throughout this paper we shall regard the jet as a small disturbance to the mean flow, so that this perturbation velocity will be irrotational, with $\boldsymbol{u} = \nabla\phi$. The potential $\phi(x, y, z, t)$ then satisfies the usual linear convected wave equation

$$-\beta^2\frac{\partial^2\phi}{\partial x^2}+\frac{\partial^2\phi}{\partial y^2}+\frac{\partial^2\phi}{\partial z^2}-\frac{1}{c_0^2}\frac{\partial^2\phi}{\partial t^2}-\frac{2M}{c_0}\frac{\partial^2\phi}{\partial x\partial t}=0, \tag{2}$$

where $\beta = (M^2-1)^{\frac{1}{2}}$, c_0 is the quiescent sound speed and M is the mean-flow Mach number ($M > 1$). Further, $\phi(x, y, z, t)$ must satisfy the following conditions:

(i) the total normal velocity on the quarter-plane must be zero, so that

$$\frac{\partial\phi}{\partial z}(x, y, 0, t)+V\delta(x-Ut)\,\delta(y-y_0)=0 \quad \text{on} \quad \{x>0, y>0\}; \tag{3}$$

(ii) owing to the symmetry of the problem, $\phi(x, y, z, t)$ must be an odd function of z, and since a pressure jump across $z = 0$ can only be supported across the rigid quarter-plane, we have that $\phi(x, y, 0, t) = 0$ except on $\{x > 0, y > 0\}$;

(iii) $\phi(x, y, z, t)$ must be causal (i.e. $\phi(x, y, z, t) = 0$ for $t < 0$), and must satisfy the radiation condition (i.e. be composed of outgoing disturbances at infinity).

We introduce the three-dimensional Fourier transform of $\phi(x, y, z, t)$, defined by

$$\Phi(k_1, k_2, z, \omega) \equiv \int_{-\infty}^{\infty}\int_{-\infty}^{\infty}\int_{-\infty}^{\infty}\phi(x, y, z, t)\exp(\mathrm{i}k_1 x+\mathrm{i}k_2 y-\mathrm{i}\omega t)\,\mathrm{d}x\,\mathrm{d}y\,\mathrm{d}t, \tag{4}$$

so that the Fourier transform of (2) becomes

$$\frac{\partial^2\Phi}{\partial z^2}-\gamma^2\Phi=0, \tag{5}$$

with $$\gamma^2(k_1, k_2, \omega) \equiv k_2^2 - \beta^2 k_1^2 + \frac{2Mk_1\omega}{c_0} - \frac{\omega^2}{c_0^2}. \tag{6}$$

Equation (5) can easily be solved, and from condition (iii) we see that

$$\Phi(k_1, k_2, z, w) = \tfrac{1}{2}\,\mathrm{sgn}\,(z)\,[\Phi(k_1, k_2, 0, \omega)]^{\pm} \exp(-\gamma|z|), \tag{7}$$

where $[\Phi(k_1, k_2, 0, \omega)]^{\pm}$ is the Fourier transform of the jump in $\phi(x, y, z, t)$ across $z = 0$, and $\gamma(k_1, k_2, \omega)$ is defined below. There must be at least two branch points (corresponding to the zeros of $\gamma(k_1, k_2, \omega)$, and possibly infinity) in each of the k_1-, k_2- and ω-planes, and the branch cuts, together with the relative positions of the contours in the subsequent Fourier inversion, are specified as follows.

(*a*) The causality condition implies that the Fourier inversion contour must pass below any singularities in the ω-plane (so that, for $t < 0$, the ω-contour can be closed in the lower half-plane to give $\phi = 0$). Further, since the radiation condition stipulates that the solution must be composed of outgoing waves, it follows that infinity is not a branch point in the ω-plane (in contrast, infinity will be a branch point in the k_1- and k_2-planes), and we therefore choose a branch cut in the ω-plane which joins the two finite branch points together; we further fix the value of γ by supposing that γ takes positive imaginary values as $\omega \to +\infty$ along the real axis.

(*b*) In the k_1-plane, given that the scattered potential upstream of the leading edge must be zero in our supersonic mean flow, both branch cuts in the k_1-plane are chosen to join to infinity through $\mathrm{Im}\,k_1 < 0$, parallel to the imaginary axis (we use the notation $\mathrm{Re}\,z$ and $\mathrm{Im}\,z$ to denote the real and imaginary parts of z respectively), and the Fourier inversion contour in the k_1-plane chosen to pass above these branch points. We suppose that γ takes negative imaginary values as $k_1 \to +\infty$ along the real axis.

(*c*) In the k_2-plane, the choice of branch cuts is also governed by the radiation condition; for $\mathrm{Re}\,\omega > 0$ we require the k_2 contour to lie below any singularities in the half-plane $\mathrm{Re}\,k_2 < 0$ and above any in the half-plane $\mathrm{Re}\,k_2 > 0$, so that in this case we choose one cut originating from the branch point in $\mathrm{Re}\,k_2 < 0$ and joining to infinity through $\mathrm{Im}\,k_2 > 0$, and another originating from the branch point in $\mathrm{Re}\,k_2 > 0$ and joining to infinity through $\mathrm{Im}\,k_2 < 0$, with both cuts running parallel to the imaginary axis; for $\mathrm{Re}\,\omega < 0$ the position of the k_2 cuts is exactly reversed. In these cases the Fourier inversion contour in the k_2-plane lies along the real axis, indented above and below the respective branch points. We note that when both k_2 branch points lie on the imaginary axis the k_2 branch cuts are chosen to lie along the imaginary axis, and the inversion contour lies along the real axis. Finally, we suppose that γ takes positive real values as $k_2 \to +\infty$ along the real axis.

We now consider the normal velocity boundary condition. Since the mean flow is supersonic, we have that $\phi(x, y, z, t)$ vanishes identically in $x < 0$, so that the transform of (3), having integrated over all values of t and positive values of x and y, becomes

$$\frac{\partial \Phi^+}{\partial z}(k_1, k_2, 0, \omega) + \frac{\mathrm{i}V \exp(\mathrm{i}k_2 y_0)}{k_1 U - \omega} = 0, \tag{8}$$

where the $+$ superfix on $\partial\Phi/\partial z$ indicates that the y-integration has been taken over the positive semi-infinite interval (that is, $0 \leqslant y < \infty$). Our method of solution will be the Wiener–Hopf technique with respect to the k_2 variable, and so at this stage we make a multiplicative factorization of $\gamma(k_1, k_2, \omega)$ in the form

$$\gamma(k_1, k_2, \omega) = \gamma^+(k_1, k_2, \omega)\,\gamma^-(k_1, k_2, \omega), \tag{9}$$

where $\gamma^{\pm}(k_1, k_2, \omega)$ are analytic, non-zero and possess algebraic behaviour at infinity in the upper and lower halves of the complex k_2-planes respectively (in what follows we denote the upper and lower k_2 half-planes by $R^{\pm}$). We find that

$$\gamma^{\pm}(k_1, k_2, \omega) = (k_2 \mp K)^{\frac{1}{2}}, \tag{10}$$

where

$$K^2 = \beta^2 k_1^2 + \frac{\omega^2}{c_0^2} - \frac{2Mk_1\omega}{c_0};$$

we take $K = \operatorname{sgn}(\omega)|K|$ when $K^2 > 0$ and $K = -\mathrm{i}|K|$ when $K^2 < 0$. Given this definition of K, together with our choice of branch cuts, it is easy to see that the factors defined in (10) have the correct analyticity properties in the respective half-planes.

The usual Wiener–Hopf equation (see Noble 1958, pp. 52–58) can now be derived by substituting (7) into (8), to yield

$$\gamma^{+}(k_1, k_2, \omega)\,[\Phi(k_1, k_2, 0, \omega)]^{\pm} + \frac{2}{\gamma^{-}(k_1, k_2, \omega)} \frac{\partial \Phi^{-}}{\partial z}(k_1, k_2, 0, \omega) - E(k_1, k_2, \omega) = 0, \tag{11}$$

where the $-$ superfix indicates that the y-integration has been performed over the negative semi-infinite y interval ($-\infty < y \leqslant 0$), so that

$$\frac{\partial \Phi}{\partial z} = \frac{\partial \Phi^{+}}{\partial z} + \frac{\partial \Phi^{-}}{\partial z},$$

and where

$$E(k_1, k_2, \omega) \equiv \frac{2\mathrm{i}V \exp(\mathrm{i}k_2 y_0)}{(k_1 U - \omega)\,\gamma^{-}(k_1, k_2, \omega)}. \tag{12}$$

The next step is to make an additive factorization of $E(k_1, k_2, \omega)$ in the form

$$E(k_1, k_2, \omega) = E^{+}(k_1, k_2, \omega) + E^{-}(k_1, k_2, \omega),$$

where $E^{\pm}(k_1, k_2, \omega)$ are analytic and possess algebraic behaviour at infinity in $R^{\pm}$ respectively. This can be completed by the use of a Cauchy integral representation of the additive factors (Noble 1958, p. 13), and we find that

$$\left.\begin{aligned} E^{-}(k_1, k_2, \omega) &= \frac{2\mathrm{i}V \exp(\mathrm{i}k_2 y_0)}{(k_1 U - \omega)\,\gamma^{-}(k_1, k_2, \omega)} \{1 - \operatorname{erf}[\exp(\tfrac{1}{4}\mathrm{i}\pi)\, y_0^{\frac{1}{2}}\, \gamma^{-}(k_1, k_2, \omega)]\}, \\ E^{+}(k_1, k_2, \omega) &= \frac{2\mathrm{i}V \exp(\mathrm{i}k_2 y_0)}{(k_1 U - \omega)\,\gamma^{-}(k_1, k_2, \omega)} \operatorname{erf}[\exp(\tfrac{1}{4}\mathrm{i}\pi)\, y_0^{\frac{1}{2}}\, \gamma^{-}(k_1, k_2, \omega)]. \end{aligned}\right\} \tag{13}$$

Full mathematical details of this derivation are presented in Appendix A, together with a demonstration of the fact that the expressions given in (13) exhibit the required analyticity properties. We now see that

$$\begin{aligned} &\gamma^{+}(k_1, k_2, \omega)\,[\Phi(k_1, k_2, 0, \omega)]^{\pm} - E^{+}(k_1, k_2, \omega) \\ &\qquad = -\frac{2}{\gamma^{-}(k_1, k_2, \omega)} \frac{\partial \Phi^{-}}{\partial z}(k_1, k_2, 0, \omega) + E^{-}(k_1, k_2, \omega); \end{aligned} \tag{14}$$

the left-hand side of (14) is analytic in R^{+} (the fact that $[\Phi(k_1, k_2, 0, \omega)]^{\pm}$ is analytic there follows from condition (ii)), and the right-hand side is analytic in R^{-}, so that by analytic continuation (14) defines a function ($f(k_2)$, say) which is analytic

throughout the complex k_2-plane. It is shown in Appendix A that $E^{\pm}(k_1, k_2, \omega) \sim k_2^{-1}$ as $k_2 \to \infty \in R^{\pm}$ respectively, and since

$$[\Phi(k_1, k_2, 0, \omega)]^{\pm}_{\mp} \sim k_2^{-\frac{3}{2}} \quad \text{as} \quad k_2 \to \infty \in R^{+}$$

and

$$\frac{\partial \Phi^{-}}{\partial z}(k_1, k_2, 0, \omega) \sim k_2^{-\frac{1}{2}} \quad \text{as} \quad k_2 \to \infty \in R^{-}$$

(these follow from the fact that the flow must be essentially incompressible, and hence satisfy Laplace's equation, close to the side edge), we see that $f(k_2) \sim k_2^{-1}$ at ∞, so that from Liouville's theorem $f(k_2) \equiv 0$, yielding two equations from (14).

We therefore have an expression for $[\Phi(k_1, k_2, 0, \omega)]^{\pm}_{\mp}$, and using the usual potential theory relation between pressure and velocity potential, together with the Fourier inversion formula, we find that the lift distribution on the plane $z = 0$ (denoted $[p(x, y, 0, t)]^{\pm}_{\mp}$) is given by

$$[p(x, y, 0, t)]^{\pm}_{\mp} = -\frac{\mathrm{i}\rho_0}{8\pi^3} \int_{\omega} \int_{k_2} \int_{k_1} \frac{E^{+}(k_1, k_2, \omega)\,(\omega - k_1 U)}{\gamma^{+}(k_1, k_2, \omega)} \exp(\mathrm{i}\omega t - \mathrm{i}k_1 x - \mathrm{i}k_2 y)\,\mathrm{d}k_1\,\mathrm{d}k_2\,\mathrm{d}\omega, \tag{15}$$

whilst the velocity potential is

$$\phi(x, y, z, t) = \frac{\operatorname{sgn}(z)}{16\pi^3} \int_{\omega} \int_{k_2} \int_{k_1} \frac{E^{+}(k_1, k_2, \omega)}{\gamma^{+}(k_1, k_2, \omega)} \times \exp(\mathrm{i}\omega t - \mathrm{i}k_1 x - \mathrm{i}k_2 y - \gamma(k_1, k_2, \omega)\,|z|)\,\mathrm{d}k_1\,\mathrm{d}k_2\,\mathrm{d}\omega. \tag{16}$$

The paths of the integration contours in (15) and (16) relative to the various branch cuts have already been chosen to satisfy the causality and radiation conditions.

3. The unsteady lift

It has not proved possible to derive a closed-form expression for the detailed unsteady lift distribution $[p(x, y, 0, z)]^{\pm}_{\mp}$, because of the complicated nature of the three-dimensional integral in (15), but we are, however, able to calculate the total (integrated) lift on the quarter-plane. We define the total life, $L(t)$, by

$$L(t) = \int_0^{\infty} \int_0^{\infty} [p(x, y, 0, t)]^{\pm}_{\mp}\,\mathrm{d}x\,\mathrm{d}y, \tag{17}$$

and from (15) (together with the fact that $[p(x, y, 0, t)]^{\pm}_{\mp}$ vanishes off the quarter-plane, so that the x- and y-integrations in (17) can be extended to $-\infty$), we rewrite (17) as

$$L(t) = -\frac{\mathrm{i}\rho_0}{8\pi^3} \int_{-\infty}^{\infty} \int_{-\infty}^{\infty} \int_{\omega} \int_{k_2} \int_{k_1} \exp(\mathrm{i}\omega t - \mathrm{i}k_1 x - \mathrm{i}k_2 y) \times \frac{E^{+}(k_1, k_2, \omega)\,(\omega - k_1 U)}{\gamma^{+}(k_1, k_2, \omega)}\,\mathrm{d}k_1\,\mathrm{d}k_2\,\mathrm{d}\omega\,\mathrm{d}x\,\mathrm{d}y. \tag{18}$$

By interchanging the orders of integration, the x- and y-integrals can be performed as $2\pi\delta(k_1)$ and $2\pi\delta(k_2)$ respectively, so that on substituting for $E^{+}(k_1, k_2, \omega)$ from (13) we find that

$$L(t) = -\frac{\rho_0 V}{\pi} \int_{\omega} \frac{\operatorname{erf}[\exp(\mathrm{i}\pi/4)\, y_0^{\frac{1}{2}} \gamma^{-}(0, 0, \omega)]}{\gamma(0, 0, \omega)} \exp(\mathrm{i}\omega t)\,\mathrm{d}\omega. \tag{19}$$

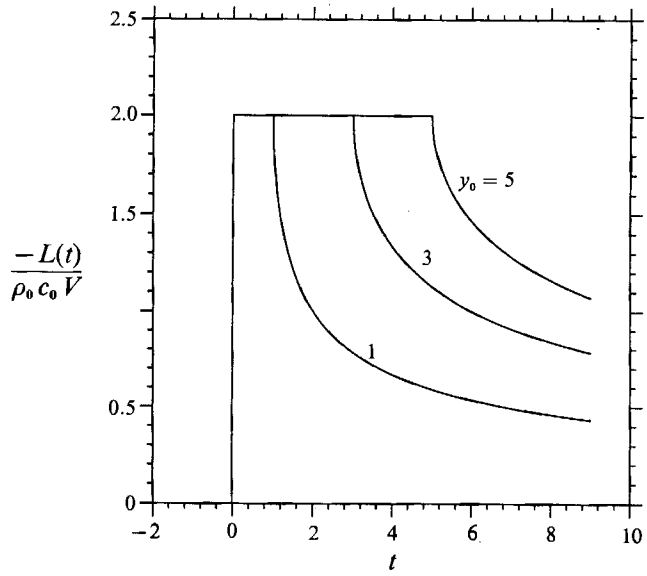

FIGURE 2. Plot of the total normalized lift on the quarter-plane, $-L(t)/(\rho_0 c_0 V)$, against time, t. The quantity y_0 takes the values 1, 3 and 5.

For $t < 0$ the integration contour in (19) is closed in the lower half-plane, yielding $L(t) = 0$. Alternatively, for $t > 0$ we seek to rewrite (19) in the form of a standard integral, and by use of the fact that $\overline{\text{erf}\,(z)} = \text{erf}\,(\bar{z})$, we have

$$L(t) = -\frac{2\rho_0 c_0 V}{\pi}\left(\int_0^\infty \text{Im}\,\frac{\exp\,(\text{i}\omega t)}{\omega}\,\text{d}\omega - J_1\right), \tag{20}$$

where

$$J_1 \equiv \int_0^\infty \text{Im}\left(\frac{\exp\,(\text{i}\omega t)}{\omega}\left\{1-\text{erf}\left[\exp\,(\text{i}\pi/4)\left(\frac{\omega y_0}{c_0}\right)^{\frac{1}{2}}\right]\right\}\right)\text{d}\omega; \tag{21}$$

it can be seen that J_1 is well-defined, since its integrand both possesses only an integrable singularity at $\omega = 0$, and approaches zero like $\omega^{-\frac{3}{2}}$ as $\omega \to \infty$. Both terms in (20) can be calculated in closed form; for $t > 0$ we have

$$\int_0^\infty \text{Im}\,\frac{\exp\,(\text{i}\omega t)}{\omega}\,\text{d}\omega = \frac{\pi}{2}, \tag{22}$$

whilst an expression for J_1 is found in Appendix B in the form

$$J_1 = \begin{cases} -\frac{1}{2}\pi & \text{if} \quad t < y_0/c_0 \\ 2\tan^{-1}\left[(tc_0/y_0)-1\right]^{\frac{1}{2}} - \frac{1}{2}\pi & \text{if} \quad t > y_0/c_0. \end{cases} \tag{23}$$

Combining these results, we therefore see from (20) that

$$L(t) = -2\rho_0 V c_0\left\{H(t) - \frac{2}{\pi}H\left(t-\frac{y_0}{c_0}\right)\tan^{-1}\left(\frac{tc_0}{y_0}-1\right)^{\frac{1}{2}}\right\}, \tag{24}$$

where $H(t)$ is the Heaviside step function. The quantity $L(t)$ is plotted in figure 2 for several values of y_0, and we see that these time histories consist of three distinct segments. First, for $t < 0$ the lift is zero, since the jet has by this time not reached the leading edge of the quarter-plane. Second, in the interval $0 < t < y_0/c_0$ the lift has

the constant value $-2\rho_0 Vc_0$; the rise from zero to this constant value occurs at $t = 0$ (i.e. when the jet first intersects the quarter-plane), and is instantaneous since the jet is compact, possessing no lengthscale. The constant value $-2\rho_0 Vc_0$ is exactly the lift experienced by a supersonic, infinite-span airfoil with infinite chord when cutting our delta-function jet, and we therefore see that in this time interval the presence of the side edge and corner has had no effect on the value of $L(t)$. In fact, $-2\rho_0 Vc_0$ is the lift that would be experienced by an infinite-span, infinite-chord airfoil cutting a circular jet of arbitrary radius but with the same volume flux as the delta-function jet (see Guo 1990). Third, for $t > y_0/c_0$ the lift decays monotonically from this constant value towards zero, only reaching zero after an infinite time, and it is clear that it is only in this time interval that the side edge and corner have any effect on the value of $L(t)$. The instant $t = y_0/c_0$ is crucial, and can be understood as follows; at $t = 0$, when the jet first intersects the quarter-plane, acoustic waves are produced, which travel at different speeds in different directions thanks to the presence of the mean flow, but it is shown in Appendix C that the time taken for these waves to first reach the side edge is exactly y_0/c_0 (the point where the waves first reach the side edge has coordinates $(My_0, 0, 0)$). At the instant when the waves reach the side edge, there will be a non-zero pressure difference between the upper and lower faces of the quarter-plane, which will induce a transverse flow from the pressure surface ($z = 0-$) to the suction surface ($z = 0+$), acting in such a way as to reduce the pressure difference between the two surfaces (and hence the total lift) to zero as $t \to \infty$. We further note that $L(t)$ is independent of the mean flow velocity, U, and this is a consequence of the flow being supersonic, since there can be no further interactions between the leading edge and the jet, once the jet has passed the leading edge.

4. The radiation

In this section we shall calculate the acoustic pressure measured by a fixed observer in the far field, but as will become apparent we shall exclude from consideration those observers lying on a single Mach-wave direction. Our starting point is the three-dimensional integral expression for the pressure, which can be simply derived from (16) in the form

$$p(x, y, z, t) = -\frac{\mathrm{i}\rho_0 \operatorname{sgn}(z)}{16\pi^3} \int_\omega \int_{k_2} \int_{k_1} C(k_1, k_2, \omega) \exp(\mathrm{i}\omega t - \mathrm{i}\psi |\boldsymbol{x}|)\, \mathrm{d}k_1\, \mathrm{d}k_2\, \mathrm{d}\omega, \quad (25)$$

where

$$C(k_1, k_2, \omega) = \frac{(\omega - k_1 U) E^+(k_1, k_2, \omega)}{\gamma^+(k_1, k_2, \omega)}, \quad (26)$$

$|\boldsymbol{x}|$ is the observer–corner separation and the phase function $\psi(k_1, k_2)$ is given by

$$|\boldsymbol{x}|\, \psi(k_1, k_2) \equiv k_1 x + k_2 y - \mathrm{i}\gamma |z|.$$

Spherical polar coordinates, centred on the origin, are defined by

$$x = |\boldsymbol{x}| \cos \Theta, \quad y = |\boldsymbol{x}| \sin \Theta \cos \chi, \quad z = |\boldsymbol{x}| \sin \Theta \sin \chi.$$

As $k_1 \to \infty$ in the upper half of the k_1-plane, we see from the arguments following (7) that

$$\gamma(k_1, k_2, \omega) \sim -\mathrm{i}\beta k_1,$$

and hence that the integrand of (25) will be exponentially small in the upper half of the k_1-plane, provided that

$$x - \beta |z| < 0; \quad (27)$$

in this case we therefore close the integration contour of the k_1-integral in the upper half-plane, yielding the result of zero pressure (since the k_1 branch cuts lie in the lower half of the k_1-plane, and the integrand possesses no poles in the k_1-plane). Condition (27) is precisely the condition for an observer to lie outside the planar Mach surface emanating from the leading edge of the quarter-plane. Inside this Mach surface (i.e. for $x-\beta|z|>0$), we shall be determining the far-field pressure by taking the limit $|x|\to\infty$ in (25) and applying the method of stationary phase to the k_1- and k_2-integrals, and in the first instance we shall therefore calculate the stationary phase points of the integral, i.e. points $k_1=\tilde{k}_1, k_2=\tilde{k}_2$ such that

$$\frac{\partial\psi}{\partial k_1}(\tilde{k}_1,\tilde{k}_2)=\frac{\partial\psi}{\partial k_2}(\tilde{k}_1,\tilde{k}_2)=0,$$

and we find that there is in fact just one stationary phase point

$$\tilde{k}_1=\frac{\omega}{\beta^2 c_0}\left[M-\frac{\cos\Theta}{(1-M^2\sin^2\Theta)^{\frac{1}{2}}}\right],\quad \tilde{k}_2=\frac{\omega\sin\Theta\cos\chi}{c_0(1-M^2\sin^2\Theta)^{\frac{1}{2}}}. \tag{28}$$

It can be shown further that

$$\left.\begin{aligned}\gamma(\tilde{k}_1,\tilde{k}_2,\omega)&=\frac{\mathrm{i}\omega\sin\Theta|\sin\chi|}{c_0(1-M^2\sin^2\Theta)^{\frac{1}{2}}},\\ \gamma^-(\tilde{k}_1,\tilde{k}_2,\omega)&=\left[\frac{\omega\sin\Theta(1+\cos\chi)}{c_0(1-M^2\sin^2\Theta)^{\frac{1}{2}}}\right]^{\frac{1}{2}},\\ \psi(\tilde{k}_1,\tilde{k}_2)&=\frac{\omega}{c_0\beta^2}[M\cos\Theta-(1-M^2\sin^2\Theta)^{\frac{1}{2}}].\end{aligned}\right\} \tag{29}$$

When $\sin\Theta>1/M$, the stationary phase point lies on the imaginary k_1- and k_2-axes and the corresponding value of $\gamma(\tilde{k}_1,\tilde{k}_2,\omega)$ is real and positive; in this case it is therefore clear that the contribution to the pressure from the stationary phase point would be exponentially small in the far field, since $p(x,y,z)$ depends on the factor $\exp(-\gamma|z|)$. We therefore see that in the region enclosed between the Mach surface $x=\beta|z|$ and the cone $\sin\Theta=1/M$ the pressure is vanishingly small in the far field, and does not correspond to the presence of propagating acoustic waves. In what follows we shall therefore consider only the region $\sin\Theta<1/M$ (i.e. inside the circular cone with its apex at the origin and semi-angle $\sin^{-1}1/M$), since it is only in this region, and for $\sin\Theta=1/M$, that the observer will receive radiation from the interaction; we shall briefly return to the question of the behaviour of the pressure for $\sin\Theta=1/M$ at the end of the next section, and merely note here that for this single value of Θ our stationary phase analysis breaks down, since the stationary phase point has become infinite.

The Hessian matrix of second partial derivatives of $\psi(k_1,k_2)$ can be found easily; when evaluated at the stationary phase point, the square root of the modulus of its determinant takes the value

$$\frac{(1-M^2\sin^2\Theta)c_0}{|\omega\sin\chi|\sin\Theta},$$

and its signature is -2 when $\omega>0$ and $+2$ when $\omega<0$. The k_1 and k_2 integrals in (25) can now be evaluated in the limit $|x|\to\infty$ (we note that the phase function, ψ, is in the correct form for application of the method of stationary phase, i.e. ψ is a *real-*

valued function multiplied by i, in the neighbourhood of the stationary phase point), and using formulae given by Jones (1966, p. 344) we find that

$$p(x,y,z,t) \sim -\frac{\mathrm{i}\rho_0 \operatorname{sgn}(z)}{8\pi^2 c_0 |x|} \int_\omega C(\tilde{k}_1, \tilde{k}_2, \omega) \frac{|\omega \sin \chi| \sin \Theta}{1-M^2 \sin^2 \Theta} \times \exp\left(\frac{\mathrm{i}\pi\omega}{(2|\omega|)}\right) \exp\left(\mathrm{i}\omega t - \mathrm{i}|x| \psi(\tilde{k}_1, \tilde{k}_2, \omega)\right) \mathrm{d}\omega, \quad (30)$$

where the factor $\exp(\mathrm{i}\pi\omega/(2|\omega|))$ has arisen from the fact that the signature of the Hessian depends on the sign of ω. We repeat that the integration contour in (30) lies along the real axis, indented below the branch points. The value of $C(\tilde{k}_1, \tilde{k}_2, \omega)$ can easily be found from (26) and (13), and it now proves convenient to write $p(x,y,z)$ as a sum of two terms in the form

$$p(x,y,z,t) \sim -\frac{\rho_0 V \operatorname{sgn}(z)}{4\pi^2 |x| (1-M^2 \sin^2 \Theta)^{\frac{1}{2}}} \int_\omega \exp(\mathrm{i}\omega \Lambda) \, \mathrm{d}\omega + \frac{\rho_0 V \operatorname{sgn}(z)}{4\pi^2 |x| (1-M^2 \sin^2 \Theta)^{\frac{1}{2}}} \int_\omega \exp(\mathrm{i}\omega \Lambda) \{1 - \operatorname{erf}[\exp(\mathrm{i}\pi/4) y_0^{\frac{1}{2}} \gamma^-(\tilde{k}_1, \tilde{k}_2, \omega)]\} \, \mathrm{d}\omega, \quad (31)$$

where $$\Lambda = t - t_1$$

and $$t_1 = \frac{|x|}{c_0 \beta^2}[M \cos \Theta - (1-M^2 \sin^2 \Theta)^{\frac{1}{2}}] - \frac{y_0 \sin \Theta \cos \chi}{c_0 (1-M^2 \sin^2 \Theta)^{\frac{1}{2}}}.$$

The integral in the first term in (31) is simply $2\pi\delta(\Lambda)$; for $t < 0$ the integration contour of the second integral in (31) is closed in the lower half of the ω-plane, to yield the value zero for the integral, whilst for $t > 0$ we rewrite the integral in the form

$$2 \operatorname{Re} \int_0^\infty \exp(\mathrm{i}\omega \Lambda) \{1 - \operatorname{erf}[\exp(\mathrm{i}\pi/4) y_0^{\frac{1}{2}} \gamma^-(\tilde{k}_1, \tilde{k}_2, \omega)]\}. \quad (32)$$

Equation (32) can be evaluated by integration by parts, in exactly the same way as is described for the integral $\mathrm{d}J_1/\mathrm{d}t$ in Appendix B, and by adding our expressions for the two terms in (31) together, we find that

$$p \sim -\frac{\rho_0 V \operatorname{sgn}(z) \delta(t-t_1)}{2\pi |x| (1-M^2 \sin^2 \Theta)^{\frac{1}{2}}} + \frac{\rho_0 V \operatorname{sgn}(z)}{2\pi^2 |x| (1-M^2 \sin^2 \Theta)^{\frac{1}{2}}} \frac{H(t-t_2) \alpha^{\frac{1}{2}}}{\Lambda |t-t_2|^{\frac{1}{2}}}, \quad (33)$$

where $$t_2 = t_1 + \alpha$$

and $$\alpha = \frac{y_0 (1+\cos \chi) \sin \Theta}{c_0 (1-M^2 \sin^2 \Theta)^{\frac{1}{2}}}.$$

We can therefore see that the radiation received by an observer in the far field, within the cone $\sin \Theta = 1/M$, is composed of two distinct signals. The first, negative pressure, signal (i.e. the first term in (33)) arrives at the observation point at the instant $t = t_1$ ($t_1 > 0$), and is exactly equal to the radiation that would have been predicted if we had considered the interaction between a delta-function jet and an infinite-span airfoil. It is easy to show (Appendix C) that the time interval t_1 is precisely the time taken for acoustic waves to propagate directly from the point where the jet first intersects the leading edge of the quarter-plane to the observer. The fact that this pressure signal is a delta function, and therefore highly singular, is purely a result of our choice of a singular (delta function) upwash on the quarter-

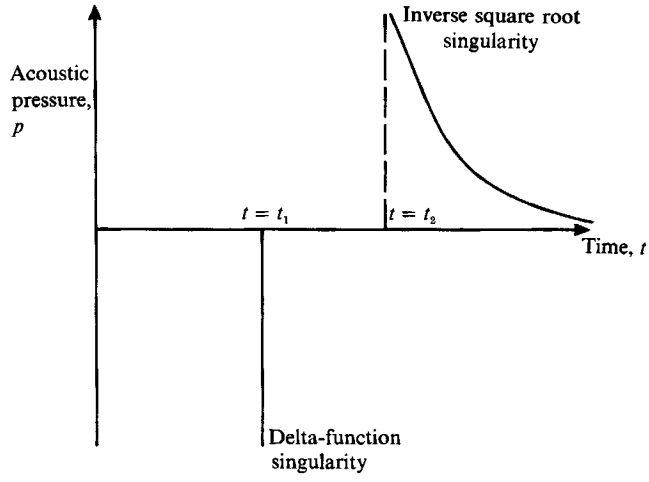

FIGURE 3. Schematic diagram of the acoustic pressure generated by the interaction between the delta-function jet and the quarter-plane. We have $|\boldsymbol{x}| = 20$, $y_0 = 5$, $M = 1.5$, $\Theta = \frac{1}{6}\pi$ and $\chi = \frac{1}{2}\pi$; the pulse at time $t = t_1$ is a delta function, and that at time $t = t_2$ is an inverse square root singularity. The jet intersects the leading edge of the quarter-plane at time $t = 0$.

plane. Since this first signal is unaffected by the presence of the corner and side edge, we conclude that the effects of the corner and side edge on the radiation are all included in the second signal (i.e. the second term in (33)), which arrives at the later time $t = t_2$. In Appendix C we demonstrate that the time interval t_2 is the least time for acoustic waves emitted from the point on the leading edge where the jet first intersects the quarter-plane to reach the side edge, be diffracted by the side edge, and then reach the observer in the far field. After the initial inverse square root singularity (again a result of the singular upwash) at $t = t_2$, this second signal, unlike the first, persists for an infinite time (since the side edge is of infinite extent, so that acoustic waves continue to be diffracted arbitrarily far from the corner), but decays towards zero amplitude as t approaches infinity. The structure of the radiation is shown schematically in figure 3.

The presence of an initial (expansion) pulse, followed by a second (compression) pulse in our problem is reminiscent of the radiation predicted by Guo (1990), who considered the interruption of a steady jet by an infinite-span, but finite-chord, airfoil in supersonic flow, and by Amiet (1986*b*), who considered the same problem for subsonic flow. In both problems it is diffraction which generates the second signal; in the Guo and Amiet problem, diffraction of acoustic waves from the leading edge by the trailing edge, and in our present problem diffraction of acoustic waves from the leading edge by the side edge. We note, however, that in the quarter-plane problem there can be no question of vortex shedding, since the mean flow is parallel to the side edge and is therefore unable to convect away any vorticity; the issue of a Kutta condition does not, therefore, arise.

The value of the analysis performed in this section has been to indicate the overall structure of the radiation, and the means by which the various components have been generated, in a relatively simple way. The singular nature of the pressure field (and hence, of the acoustic intensity and energy) is of course unphysical, and, as emphasized above, has resulted from our original choice of the delta-function upwash distribution. Since both signals in the radiation are singular, it is not possible to compare the relative magnitudes of the effects of the leading and side edges on the

radiation; in the next section, however, we go on to consider a more realistic, diffuse, upwash distribution, which will have the effect of producing a 'smoothed-out', non-singular version of (33), in which the magnitude of the two signals can be compared.

5. Diffuse jet velocity

In the previous two sections we have considered the interaction between the quarter-plane and a highly compact jet, represented by a delta function, and, not surprisingly, the use of such a singular upwash distribution led to the presence of singularities (a delta function and an inverse square root singularity) in the radiated field. In this section we therefore consider how the radiation is modified when we take account of the fact that real vortex cores are not totally compact, but rather possess their own non-zero lengthscale; that is to say, we shall consider a more diffuse distribution of the jet velocity normal to the quarter-plane. We start by replacing the delta-function upwash in (1) by the expression

$$\frac{V}{\pi a^2}\exp\left[-\frac{(x-Ut)^2}{a^2}-\frac{(y-y_0)^2}{a^2}\right]z, \tag{34}$$

i.e. the upwash on the quarter-plane is supposed to possess a Gaussian distribution, with characteristic lengthscale a, which is precisely the form of the upwash applied by Amiet (1986*b*). We note that the volume flux transported by a jet with axial velocity distribution (34), obtained by integrating (34) across the plane $z = 0$, is equal to that of the delta-function jet in (1) (i.e. equal to V), and further that in the limit $a \to 0$ equation (34) reduces exactly to (1) (see Jones 1966, p. 51). We shall suppose that $a \ll y_0$, in recognition of the fact that the tip vortices from high-speed propellers are likely to be tightly rolled up, so that in effect we are supposing that the centre of the jet intersects the leading edge at some distance from the corner.

The analysis proceeds in much the same way as in §§2 and 4. The normal velocity boundary condition, (3), becomes

$$\frac{\partial\phi}{\partial z}(x,y,0,t)+\frac{V}{\pi a^2}\exp\left[-\frac{(x-Ut)^2}{a^2}-\frac{(y-y_0)^2}{a^2}\right]=0 \quad \text{on} \quad \{x>0, y>0\}; \tag{35}$$

as before, we now use the fact that the scattered field vanishes in $x < 0$, and Fourier transform (35) over the infinite t-interval and over the positive semi-infinite x- and y-intervals, so that the transform of the second term in (35) is

$$\frac{V}{\pi a^2}\int_{-\infty}^{\infty}\int_0^{\infty}\int_0^{\infty}\exp\left[-\frac{(x-Ut)^2}{a^2}-\frac{(y-y_0)^2}{a^2}\right]\exp\left(\mathrm{i}k_1 x+\mathrm{i}k_2 y-\mathrm{i}\omega t\right)\mathrm{d}y\,\mathrm{d}x\,\mathrm{d}t. \tag{36}$$

Since we have $a \ll y_0$, so that $\exp(-y_0^2/a^2) \ll 1$, the lower limit in the y-integral can be replaced by $-\infty$, as the integrand of (36) will be exponentially small in $y < 0$. This approximation is equivalent to supposing that when the jet first reaches the quarter-plane, it interacts principally with the leading edge, and its initial interaction with the side edge is very weak; or alternatively, that at sufficiently late times almost all the jet momentum flux across $z = 0$ is incident on the quarter-plane. Once this approximation has been made the analysis proceeds in exactly the same way as in §2, and the Wiener–Hopf equation in this case turns out to be identical to (11), except that $E(k_1, k_2, \omega)$ defined in (12) is replaced by $F(k_1, k_2, \omega)$, where

$$F(k_1,k_2,\omega)\equiv\frac{2\mathrm{i}V\exp\left[\mathrm{i}k_2 y_0-(\omega^2a^2/4U^2)-\frac{1}{4}k_2^2a^2\right]}{(k_1U-\omega)\gamma^-(k_1,k_2,\omega)}; \tag{37}$$

the effect of considering the diffuse jet velocity distribution given by (34) has been to introduce the Gaussian factors seen in (37).

The solution is now completed by making an additive factorization of $F(k_1, k_2, \omega)$ in the form

$$F(k_1, k_2, \omega) = F^+(k_1, k_2, \omega) + F^-(k_1, k_2, \omega),$$

where $F^\pm(k_1, k_2, \omega)$ are analytic and possess algebraic behaviour at infinity in $R^\pm$ respectively. This factorization is again performed using the Cauchy integral representation of $F^\pm$; we have that

$$F^-(k_1, k_2, \omega) = \frac{2\mathrm{i}V \exp(-\omega^2 a^2/4U^2)}{k_1 U - \omega} \left\{ \frac{-1}{2\pi\mathrm{i}} \int_\xi \frac{\exp(\mathrm{i}\xi y_0 - \frac{1}{4}\xi^2 a^2)}{\gamma^-(k_1, \xi, \omega)(\xi - k_2)} \mathrm{d}\xi \right\}, \tag{38}$$

with the integration contour being the real axis indented above the pole at $\xi = k_2$, and in order to facilitate calculation of the integral in (38) we make the approximation

$$\exp(-\tfrac{1}{4}\xi^2 a^2) \approx (1 + \tfrac{1}{4}\xi^2 a^2)^{-1}, \tag{39}$$

which is valid on the real axis, and hence along the integration contour of (38) (this method of approximating the Wiener–Hopf kernel in order to facilitate its factorization is due to Koiter (1954), and is described by Noble (1958, p. 160)). Of course, we could have applied this approximation to the Gaussian throughout the analysis, for instance in the original upwash distribution in (34), and not just in determining the additive Wiener–Hopf factors. However, it has proved desirable to retain rapid exponential decay at infinity at certain points in the argument (for instance, in extending the lower limit of the integral in (36) to $-\infty$, and in enhancing the convergence properties of an integral which must be calculated numerically – see (48)). Moreover, it seems appropriate to apply approximation (39) only in that part of the present analysis in which it has previously been shown to yield good results, and that is precisely in the calculation of the Wiener–Hopf factors.

From (38), $F^-(k_1, k_2, \omega)$ is therefore given in this approximation by

$$F^-(k_1, k_2, \omega) = -\frac{V}{\pi(k_1 U - \omega)} \exp(-\omega^2 a^2/4U^2) I_2, \tag{40}$$

where the integral I_2 is defined by

$$I_2 \equiv \int_\xi \frac{\exp(\mathrm{i}\xi y_0)}{\gamma^-(k_1, \xi, \omega)(\xi - k_2)(1 + \frac{1}{4}\xi^2 a^2)} \mathrm{d}\xi; \tag{41}$$

the derivation of a closed-form expression for I_2 is given in Appendix D. Substituting the result from (D 3) into (40), we find that $F^-(k_1, k_2, \omega)$ is given by

$$\begin{aligned} F^-(k_1, k_2, \omega) = {} & \frac{2\mathrm{i}V \exp(-\omega^2 a^2/4U^2)}{k_1 U - \omega} \\ & \times \left\{ \frac{\exp(\mathrm{i}k_2 y_0)\{1 - \mathrm{erf}[\exp(\frac{1}{4}\mathrm{i}\pi) y_0^{\frac{1}{2}} \gamma^-(k_1, k_2, \omega)]\}}{\gamma^-(k_1, k_2, \omega)(1 + \frac{1}{4}k_2^2 a^2)} \right. \\ & + \frac{\exp(-2y_0/a)\,\mathrm{erf}[\exp(\frac{1}{4}\mathrm{i}\pi) y_0^{\frac{1}{2}} \gamma^-(k_1, 2\mathrm{i}/a, \omega)]}{\gamma^-(k_1, 2\mathrm{i}/a, \omega)(\mathrm{i}ak_2 + 2)} \\ & \left. + \frac{\exp(2y_0/a)\{1 - \mathrm{erf}[\exp(\frac{1}{4}\mathrm{i}\pi) y_0^{\frac{1}{2}} \gamma^-(k_1, -2\mathrm{i}/a, \omega)]\}}{\gamma^-(k_1, -2\mathrm{i}/a, \omega)(\mathrm{i}ak_2 - 2)} \right\}, \end{aligned} \tag{42}$$

and an expression for $F^+(k_1, k_2, \omega)$ can be found from $F^+ = F - F^-$. It is easy to see that the expression given in (42) possesses the desired analyticity properties in R^-; the only possible singularity of (42) in R^- is at $k_2 = -2\mathrm{i}/a$, but we note that the second term in the large curly brackets is analytic in R^- anyway, and that the first and third terms combine so that the residue at $k_2 = -2\mathrm{i}/a$ is zero; whilst the fact that (42) decays algebraically as $k_2 \to \infty \in R^-$ follows in exactly the same way as in Appendix A (this is essentially because the exponential decay of the complementary error function in the first term of (42) as $k_2 \to \infty \in R^-$ is exactly balanced by the exponential growth of the factor $\exp(\mathrm{i}k_2 y_0)$). It is possible to make some further simplification of (42), however, using the fact that we are supposing a to be small; in this case

$$[\gamma^-(k_1, \pm 2\mathrm{i}/a, \omega)]^2 \sim \pm 2\mathrm{i}/a \quad \text{as} \quad a \to 0 \tag{43}$$

and we can apply the large-argument form of the error function (equation (A 7)) to the second and third terms in (42), to yield an approximate expression for $F^-(k_1, k_2, \omega)$ in the form

$$\begin{aligned} F^-(k_1, k_2, \omega) = {} & \frac{2\mathrm{i}V \exp(-\omega^2 a^2/4U^2)}{k_1 U - \omega} \\ & \times \left\{ \frac{\exp(\mathrm{i}k_2 y_0)}{\gamma^-(k_1, k_2, \omega)(1 + \frac{1}{4}a^2 k_2^2)} \{1 - \mathrm{erf}[\exp(\tfrac{1}{4}\mathrm{i}\pi) y_0^{\frac{1}{2}} \gamma^-(k_1, k_2, \omega)]\} \right. \\ & \left. + a \frac{\exp(\frac{1}{4}\mathrm{i}\pi)}{(4\pi y_0)^{\frac{1}{2}}} \left(\frac{1}{\mathrm{i}ak_2 + 2} + \frac{1}{\mathrm{i}ak_2 - 2} \right) \right\}; \end{aligned} \tag{44}$$

by setting $a = 0$ we can see that this reduces to the expression for $E^-(k_1, k_2, \omega)$ given in (13). Now that $F(k_1, k_2, \omega)$ has been decomposed, the determination of the radiation proceeds in exactly the same way as it did in §4 for the delta-function jet. We find that the acoustic pressure in this case is again given by (25), but with the quantity $C(k_1, k_2, \omega)$ defined in (26) replaced by

$$D(k_1, k_2, \omega) = \frac{(\omega - k_1 U) F^+(k_1, k_2, \omega)}{\gamma^+(k_1, k_2, \omega)}. \tag{45}$$

The radiation in the far field is again determined by the method of stationary phase in the limit $|\boldsymbol{x}| \to \infty$, and just as in §4, equation (30), we find that

$$\begin{aligned} p(x, y, z, t) \sim {} & -\frac{\mathrm{i}\rho_0 \operatorname{sgn}(z)}{8\pi^2 c_0 |\boldsymbol{x}|} \int_\omega D(\tilde{k}_1, \tilde{k}_2, \omega) \frac{|\omega \sin\chi| \sin\Theta}{1 - M^2 \sin^2\Theta} \\ & \times \exp\left(\frac{\mathrm{i}\pi\omega}{2|\omega|}\right) \exp(\mathrm{i}\omega t - \mathrm{i}|\boldsymbol{x}| \psi(\tilde{k}_1, \tilde{k}_2, \omega)) \, \mathrm{d}\omega, \end{aligned} \tag{46}$$

with $\tilde{k}_{1,2}$ as previously defined, and the path of integration in the ω-plane again corresponding to the real axis, indented below any branch points.

In order to study (46) we will for simplicity take the case of an observer with $\chi = \frac{1}{2}\pi$ (i.e. an observer positioned directly above the side edge, as is done by Amiet 1986*b* and Guo 1990), in which case $\tilde{k}_2 = 0$ and the second term in the large curly brackets in (44) vanishes, and we find that

$$F^+(\tilde{k}_1, \tilde{k}_2, \omega) = \frac{2\mathrm{i}V \exp(-\omega^2 a^2/4U^2)}{(\tilde{k}_1 U - \omega)\gamma^-(\tilde{k}_1, 0, \omega)} \mathrm{erf}[\exp(\tfrac{1}{4}\mathrm{i}\pi) y_0^{\frac{1}{2}} \gamma^-(\tilde{k}_1, 0, \omega)]. \tag{47}$$

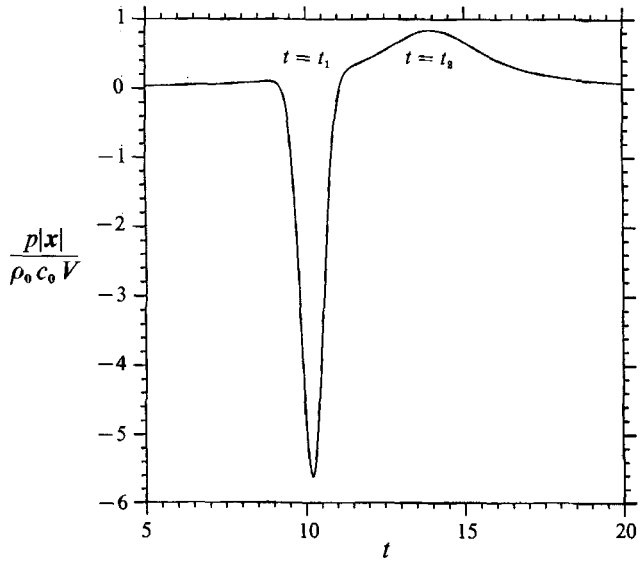

FIGURE 4. The acoustic pressure generated by the interaction between the Gaussian jet and the quarter-plane, for a fixed observer position. The quantity plotted is $p|x|/(\rho_0 c_0 V)$ against time, and we have $a = 0.75$, $y_0 = 5$, with other parameters as in figure 3.

By substituting (47) and (45) into (46) we therefore obtain an expression for the pressure in the plane $\chi = \frac{1}{2}\pi$, which we write in the form

$$p(x,y,z) = -\frac{\rho_0 V \operatorname{sgn}(z)}{4\pi^2|x|(1-M^2\sin^2\Theta)^{\frac{1}{2}}}\int_\omega \exp(\mathrm{i}\omega\Lambda)\exp(-\omega^2a^2/4U^2)\,\mathrm{d}\omega$$
$$+\frac{\rho_0 V \operatorname{sgn}(z)}{4\pi^2|x|(1-M^2\sin^2\Theta)^{\frac{1}{2}}}\int_\omega \exp(\mathrm{i}\omega\Lambda)\{1-\operatorname{erf}[\exp(\tfrac{1}{4}\mathrm{i}\pi)y_0^{\frac{1}{2}}\gamma^-(\tilde{k}_1,0,\omega)]\}$$
$$\times\exp\left(-\frac{\omega^2a^2}{4U^2}\right)\mathrm{d}\omega. \tag{48}$$

Comparing (48) and (31), we see that the effect of the inclusion of the Gaussian jet velocity distribution on the pressure in the far field for $\chi = \frac{1}{2}\pi$ (equation (48)) has been to introduce the additional factor $\exp(-\omega^2a^2/4U^2)$ into the equivalent expression for the delta-function jet radiation (equation (31)); by taking the limit $a \to 0$, (48) reduces to (31). The first integral in (48) can easily be evaluated as

$$(2U\,\pi^{\frac{1}{2}}/a)\exp(-\Lambda^2U^2/a^2);$$

unlike the delta-function jet case of §4, however, it has not proved possible to find a closed-form expression for the second integral in (48), but a numerical calculation can easily be performed, and the results are presented below.

In figure 4 we plot the dimensional quantity $p|x|/(\rho_0 c_0 V)$, computed from (48), against time for a fixed observer position in the far field. This time history clearly consists of two distinct signals, just as in figure 3 for the delta-function jet, but here, following our choice of a smooth upwash distribution, the plot is infinitely differentiable. The first signal, with its maximum amplitude occurring at time $t \approx 10$ (i.e. at time $t = t_1$ in the notation of the previous section), represents the radiation which, having been generated by the interaction between the jet and the leading edge, has propagated directly to the observer; this corresponds to the first term in

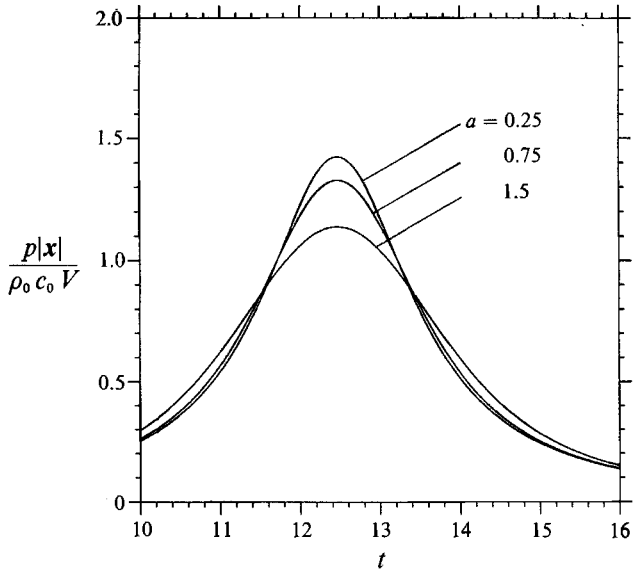

FIGURE 5. Plot of that part of the acoustic pressure resulting from diffraction of sound by the side edge (i.e. the second term in (48)), for various values of a (the Gaussian lengthscale), with $y_0 = 3$ and other parameters as in figure 3.

(48). Alternatively, the second signal, with maximum amplitude at time $t \approx 14$ (i.e. at $t = t_2$), represents radiation generated at the leading edge which has subsequently been diffracted by the side edge before reaching the observer; this corresponds to the second term in (48). We note in particular that the first signal possesses both a very much greater amplitude and a shorter duration than the second. We also note that the two signals possess opposite signs (given our original choice of jet velocity direction, the initial signal for observers above the quarter-plane is negative), and in fact the t-integral of the acoustic pressure over the interval $-\infty < t < \infty$, for both this Gaussian jet and the delta-function jet, is exactly zero. This can be seen from (46) (and (30) in the delta-function jet case) by taking the t-integrals of (46) and (30), and exchanging the orders of integration so that the t-integrals reduce to $2\pi\delta(\omega)$; the value of the integrated pressure now depends on the value of the integrand at $\omega = 0$, which can be shown to be zero for both (46) and (30). The fact that $\int p\,dt$ vanishes can be checked directly in the delta-function jet case by integration of (33) with respect to time. This result was also found by Guo (1990) for the interruption of a circular jet by a finite-chord, but infinite-span, airfoil.

In figure 5, only the second (diffracted) signal is plotted for various values of the jet lengthscale a; we note how, as a is decreased, the amplitude of the signal increases and the duration decreases, which is exactly as expected, since the formal limit $a \to 0$ applied to the Gaussian jet yields our original delta-function jet, the radiation of which was seen to possess an inverse square root singularity at time $t = t_2$. We emphasize, however, that for each value of a considered in figure 5, the first signal (not shown) is considerably larger, and indeed that this first signal grows much more rapidly than the second as a is reduced.

As has already been noted, in the limit $a \to 0$ the Gaussian jet reduces exactly to the delta-function jet of (1). It is easy to calculate the momentum and kinetic energy fluxes of the Gaussian jet across the plane $z = 0$, which turn out to be

$$\rho_0 V^2/2\pi a^2 \quad \text{and} \quad \rho_0 V^3/3\pi^2 a^4$$

respectively; hence, we can see by taking the limit $a \to 0$ that the momentum and energy fluxes of the delta-function jet are infinite. The infinity in the incident energy explains the fact that the time-integral of the acoustic energy density (which is essentially proportional to the square of the pressure) is divergent in the delta-function jet case; it is easy to see that the integrated energy density is divergent, due to the presence in the pressure (equation (33)) of both the delta function at $t = t_1$ (a product of two delta functions is non-integrable) and the inverse square root singularity at $t = t_2$ (which, when squared, gives a non-integrable $(t-t_2)^{-1}$ singularity in the energy density). However, for the Gaussian jet (with $a \neq 0$), the energy transported into the system by the jet is clearly finite, and there are no problems of non-convergence in the total radiated energy.

We can see from (33) and (48) that the acoustic pressure measured by observers lying inside the cone $\sin \Theta = 1/M$ decays with distance according to $1/|x|$, i.e. due to spherical spreading. Such a conclusion cannot immediately be drawn for $\sin \Theta = 1/M$, however, since the expressions for the radiation in (33) and (48) become singular, thanks to the presence of the factor $1/(1-M^2 \sin^2 \Theta)^{\frac{1}{2}}$. This singularity has arisen in our analysis due to the failure of the method of stationary phase (from (28) we see that the stationary phase point lies at infinity for this particular value of Θ), but this difficulty could in part be remedied by transforming coordinates into the jet rest frame (i.e. the frame in which the quarter-plane is moving through still fluid), which is the approach adopted by Ffowcs Williams & Guo (1988) and Guo (1990). If this were done, then the stationary phase analysis could be applied for $\sin \Theta = 1/M$ as well, except for an observer lying along the single azimuthal direction $\chi = \frac{1}{2}\pi$, again leading to the pressure being inversely proportional to observer distance. It can therefore be concluded that, apart from along the unique observer direction $\sin \Theta = 1/M, \chi = \frac{1}{2}\pi$, the pressure decays with observer distance due to spherical spreading; the analysis for this simple extension of our present results will not be presented here. Turning now to the single direction $\sin \Theta = 1/M$, $\chi = \frac{1}{2}\pi$ in our blade rest frame (corresponding to the Mach-wave direction in Ffowcs Williams & Guo's jet rest frame), we note that in the case of an infinite-span airfoil and a circular jet, Ffowcs Williams & Guo (1988) have shown that an intense pressure pulse is launched along this Mach-wave direction, which, according to linear theory, reaches the far field unattenuated (i.e. its amplitude does not decay at all with distance). In the interaction between a jet and a quarter-plane, such a feature must inevitably also be present; indeed, in the case of a circular jet, the Mach-wave pulse from the leading-edge interaction must be exactly equal to that predicted by Ffowcs Williams & Guo, since no signal from the side edge can catch up with it (always provided that the path of the jet does not lie so close to the corner that the jet intersects the leading edge and side edge simultaneously). It does not seem possible at present to extract this behaviour along the Mach-wave direction from the complicated integrals in (46), but as argued above this intense pulse, launched from the leading edge, seems to be independent of the presence of the corner, and for a given jet velocity distribution could presumably be investigated using the techniques for an infinite-span airfoil described by Ffowcs Williams & Guo (1988).

6. Concluding remarks

In this paper we have considered the lift and radiation generated when a rigid quarter-plane lying in supersonic mean flow intersects a perpendicular velocity jet convected by the mean flow, which is a model problem of relevance to the question

of tip-vortex interaction noise produced by modern propellers. The essential extension which this analysis represents over previous work lies in our choice of a quarter-plane airfoil, in order to better represent the effects of the blade tip.

The time histories of the lift and radiation have been calculated, and the various features explained by consideration of standard retarded-time arguments. Regarding the lift, the presence of the side edge was seen to cause the lift to decay towards zero, but only once acoustic waves generated at the leading edge had first reached the side edge. Since modern propeller blades will typically have long chords, it does seem likely that the sort of variation in the unsteady lift on an individual blade predicted in §3 would occur in practice, because the rear-row blades would not have completely passed through the vortex core before waves from the leading-edge interaction had reached the blade tip. It therefore seems that an infinite-span airfoil calculation could substantially overestimate the level of unsteady loading generated by the tip vortices on the rear blades. Regarding the radiation in our simplified rectilinear-motion problem, the far-field acoustic pressure has been seen to be composed of two signals; the first, relatively intense, signal from the leading-edge–jet interaction, and a second signal of the opposite sign and with a smaller amplitude and longer duration, arising from the diffraction of leading-edge sound by the side edge. Whilst it is of course this second signal which is a particular feature of our quarter-plane problem, it is also clear that it is the first signal which would be the more subjectively annoying noise component in practical terms.

The author is particularly grateful for the financial support provided by Emmanuel College, Cambridge.

Appendix A

In this appendix we consider the additive factorization of the function $E(k_1, k_2, \omega)$ in the form

$$E(k_1, k_2, \omega) = E^+(k_1, k_2, \omega) + E^-(k_1, k_2, \omega), \tag{A 1}$$

where $E(k_1, k_2, \omega)$ is defined by

$$E(k_1, k_2, \omega) \equiv \frac{2\mathrm{i}V \exp(\mathrm{i}k_2 y_0)}{(k_1 U - \omega)\gamma^-(k_1, k_2, \omega)}, \tag{A 2}$$

and where $E^\pm(k_1, k_2, \omega)$ are analytic and possess algebraic behaviour at infinity in the upper and lower halves of the complex k_2-plane respectively. Although the expression in (A 2) is analytic throughout the lower half-plane, it possesses exponential growth as $k_2 \to -\mathrm{i}\infty$, so that the factorization is certainly non-trivial.

Integral expressions for $E^\pm(k_1, k_2, \omega)$ are given by Noble (1958, p. 13), and we have, for instance, that

$$E^-(k_1, k_2, \omega) = -\frac{1}{2\pi\mathrm{i}}\left(\frac{2\mathrm{i}V}{k_1 U - \omega}\right)\int_\xi \frac{\exp(\mathrm{i}\xi y_0)}{(\xi - k_2)\gamma^-(k_1, \xi, \omega)}\mathrm{d}\xi, \tag{A 3}$$

with the integration contour lying along the real axis, but indented above the pole at $\xi = k_2$. We close the contour in the upper half of the ξ-plane, leaving a branch-line integral, and find that

$$E^-(k_1, k_2, \omega) = \frac{2V \exp(\frac{3}{4}\pi\mathrm{i} - \mathrm{i}Ky_0)}{\pi(k_1 U - \omega)} I_1, \tag{A 4}$$

where
$$I_1 \equiv \int_0^\infty \frac{\exp(-ry_0)\,\mathrm{d}r}{r^{\frac{1}{2}}[r+\mathrm{i}(K+k_2)]}, \tag{A 5}$$

and where K has been previously defined following (10). The integral I_1 can be determined by making the substitution $r = t^2$ and using results from Abramowitz & Stegun (1968) (p. 297, §§7.1.3, 7.1.4), and we find that

$$E^-(k_1, k_2, \omega) = \frac{2\mathrm{i}V\exp(\mathrm{i}k_2 y_0)}{(k_1 U-\omega)\gamma^-(k_1, k_2, \omega)}\{1-\mathrm{erf}[\exp(\tfrac{1}{4}\mathrm{i}\pi)\, y_0^{\frac{1}{2}}\gamma^-(k_1, k_2, \omega)]\}, \tag{A 6}$$

where the error function erf (z) is defined by

$$\mathrm{erf}(z) = \frac{2}{\pi^{\frac{1}{2}}}\int_0^z \exp(-u^2)\,\mathrm{d}u. \tag{A 7}$$

It is easy to see that

$$\begin{aligned} E^+(k_1, k_2, \omega) &= E(k_1, k_2, \omega) - E^-(k_1, k_2, \omega) \\ &= \frac{2\mathrm{i}V\exp(\mathrm{i}k_2 y_0)}{(k_1 U-\omega)\gamma^-(k_1, k_2, \omega)}\,\mathrm{erf}[\exp(\tfrac{1}{4}\mathrm{i}\pi)\, y_0^{\frac{1}{2}}\gamma^-(k_1, k_2, \omega)]. \end{aligned} \tag{A 8}$$

The expressions for $E^\pm(k_1, k_2, \omega)$ given in (A 6) and (A 8) have the desired analyticity properties and behaviour at infinity; the expression for $E^-(k_1, k_2, \omega)$ in (A 6) is clearly analytic in R^-, whilst the analyticity of (A 8) throughout R^+ is guaranteed by the fact that the function erf $(z)/z$ is analytic at $z = 0$ (so that E^+ is analytic at the zero of γ^- in R^+); in addition, using the result (Abramowitz & Stegun 1968, p. 298)

$$1-\mathrm{erf}(z) \sim \frac{1}{\pi^{\frac{1}{2}}z}\exp(-z^2) \quad \text{as} \quad z\to\infty, \tag{A 9}$$

we see that in (A 6) and (A 8)

$$E^\pm(k_1, k_2, \omega) \sim k_2^{-1} \quad \text{as} \quad k_2\to\infty\in R^\pm, \tag{A 10}$$

so that our expressions for $E^\pm$ have the required algebraic behaviour at infinity.

Appendix B

In this appendix we derive an expression for the integral J_1, defined by

$$J_1 \equiv \int_0^\infty \mathrm{Im}\left(\frac{\exp(\mathrm{i}\omega t)}{\omega}\left\{1-\mathrm{erf}\left[\exp(\tfrac{1}{4}\mathrm{i}\pi)\left(\frac{\omega y_0}{c_0}\right)^{\frac{1}{2}}\right]\right\}\right)\mathrm{d}\omega. \tag{B 1}$$

We have that

$$\frac{\mathrm{d}J_1}{\mathrm{d}t} = \mathrm{Re}\int_0^\infty\left[1-\mathrm{erf}\left(\frac{\mathrm{i}y_0\omega}{c_0}\right)^{\frac{1}{2}}\right]\exp(\mathrm{i}\omega t)\,\mathrm{d}\omega, \tag{B 2}$$

and performing this integral by parts we find that

$$\frac{\mathrm{d}J_1}{\mathrm{d}t} = \mathrm{Re}\left\{\frac{\exp(-\mathrm{i}\sigma-\frac{1}{2}\mathrm{i}\pi)}{t}\left|1-\frac{c_0 t}{y_0}\right|^{-\frac{1}{2}}\right\}, \tag{B 3}$$

where $\sigma = -\frac{1}{2}\pi$ when $t - y_0/c_0 > 0$ and $\sigma = 0$ when $t - y_0/c_0 < 0$.

J_1 can now be recovered by integrating (B 3) with respect to t; we note that $\mathrm{d}J_1/\mathrm{d}t = 0$ for $t < y_0/c_0$, so that

$$J_1 = C_1 \quad \text{when} \quad t < y_0/c_0, \tag{B 4}$$

where C_1 is a constant. Alternatively, we find that

$$J_1 = 2\tan^{-1}[(c_0 t/y_0)-1]^{\frac{1}{2}} + C_2 \quad \text{when} \quad t > y_0/c_0, \tag{B 5}$$

where C_2 is also a constant. The value of C_2 can be found by considering the limiting value of J_1 as $t \to \infty$; we see that in the limit $t \to \infty$ the integrand in (B 1) oscillates rapidly, and in order to find the asymptotic form of J_1 in the limit $t \to \infty$ we can therefore approximate the integrand of J_1 by its value in the neighbourhood of $\omega = 0$, so that from (B 1)

$$J_1 \sim \int_0^\infty \frac{\sin \omega t}{\omega}\,\mathrm{d}\omega - 2\left(\frac{y_0}{\pi c_0}\right)^{\frac{1}{2}} \int_0^\infty \frac{\sin(\omega t + \frac{1}{4}\pi)}{\omega^{\frac{1}{2}}}\,\mathrm{d}\omega. \tag{B 6}$$

The second integral in (B 6) tends to zero like $t^{-\frac{1}{2}}$ as $t \to \infty$, so that $J_1 \sim \frac{1}{2}\pi$ as $t \to \infty$. Hence, from (B 5) we have that $C_2 = -\frac{1}{2}\pi$, and by the continuity of $L(t)$ at $t = y_0/c_0$, we have further that $C_1 = -\frac{1}{2}\pi$ as well.

Appendix C

In this appendix we derive expressions for the time taken for acoustic signals to propagate between various fixed observer positions in the uniform mean flow. Defining spherical polar coordinates centred on the origin as in §4, the time taken for a signal emitted from the origin to first reach the point with spherical polar coordinates (r, Θ, χ) is

$$\frac{r}{c_0\beta^2}\{M\cos\Theta - (1-M^2\sin^2\Theta)^{\frac{1}{2}}\}; \tag{C 1}$$

this is clear from Dowling & Ffowcs Williams' (1983, p. 191ff) retarded-time arguments concerning a source in supersonic motion. We consider only observer positions for which $\sin\Theta < 1/M$. If we now use a different set of spherical coordinates (r', Θ', χ'), this time centred on the point $(x = z = 0,\ y = y_0)$, so that

$$\left.\begin{aligned} r'\cos\Theta' = r\cos\Theta, \quad r'\sin\Theta'\cos\chi' = r\sin\Theta\cos\chi - y_0, \\ r'\sin\Theta'\sin\chi' = r\sin\Theta\sin\chi, \end{aligned}\right\} \tag{C 2}$$

we see from (C 1) that the time taken for an acoustic signal to travel from the point on the leading edge (i.e. the line $x = z = 0$) at $y = y_0$ to the point with spherical polar coordinates (r, Θ, χ) relative to the origin is

$$\tau = (1/c_0\beta^2)\{Mr\cos\Theta - [r^2(1-M^2\sin^2\Theta) - \beta^2(y_0^2 - 2ry_0\sin\Theta\cos\chi)]^{\frac{1}{2}}\}. \tag{C 3}$$

If we choose $\Theta = 0$ (i.e. a point on the side edge $y = z = 0$) and $x = X$, then

$$\tau = (1/c_0\beta^2)\{MX - (X^2 - \beta^2 y_0^2)^{\frac{1}{2}}\}; \tag{C 4}$$

the expression in (C 4) is just the time taken for an acoustic signal emitted from the point where the delta-function jet intersects the leading edge to first reach the point $x = X$ on the side edge; treating τ as a function of X, it is easy to see that the

minimum value of τ for varying X is y_0/c_0, and that this minimum occurs for $X = My_0$. Therefore, signals emitted from the point at which the jet intersects the leading edge first reach the side edge after an interval of time equal to y_0/c_0.

In the same way, the time taken for a signal emitted from the point $(x = X, y = z = 0)$ to first reach the point with spherical polar coordinates (r, Θ, χ) relative to the origin can be shown from (C 1) to be

$$(1/c_0\beta^2)\{M(r\cos\Theta - X) - (r^2 + X^2 - 2rX\cos\Theta - M^2r^2\sin^2\Theta)^{\frac{1}{2}}\}, \tag{C 5}$$

so that the total time, τ', for a wave first emitted from $(y = y_0, x = z = 0)$ to travel to $(x = X, y = z = 0)$, and then to be diffracted by the side edge and reach the point with spherical polar coordinates relative to the origin (r, Θ, χ) in the far field (i.e. $r \gg 1$) is obtained by adding (C 4) and (C 5), and is given by

$$\tau' = \frac{1}{c_0\beta^2}\left\{Mr\cos\Theta - (X^2 - \beta^2 y_0^2)^{\frac{1}{2}} - r(1 - M^2\sin^2\Theta)^{\frac{1}{2}} + \frac{X\cos\Theta}{(1 - M^2\sin^2\Theta)^{\frac{1}{2}}}\right\} + O(r^{-1}). \tag{C 6}$$

Treating τ' as a function of X, the minimum value of τ' is found to be

$$\frac{1}{c_0\beta^2}\left\{Mr\cos\Theta - r(1 - M^2\sin^2\Theta)^{\frac{1}{2}} + \frac{y_0\beta^2\sin\Theta}{(1 - M^2\sin^2\Theta)^{\frac{1}{2}}}\right\}, \tag{C 7}$$

which occurs for $X = y_0\cot\Theta$. We therefore see that the time taken for the disturbance caused by the intersection of the jet with the leading edge to reach the side edge and then to first reach a particular point in the far field is given by (C 7). Alternatively, the time taken for the disturbance to propagate directly from the leading edge to the far field can be found from (C 3), and is

$$\frac{r}{c_0\beta^2}[M\cos\Theta - (1 - M^2\sin^2\Theta)^{\frac{1}{2}}] - \frac{y_0\sin\Theta\cos\chi}{c_0(1 - M^2\sin^2\Theta)^{\frac{1}{2}}}. \tag{C 8}$$

Appendix D

In this appendix we derive an expression for the integral I_2, defined in (41), and written here in a slightly different form as

$$I_2 \equiv \frac{4}{a^2}\int_\xi \frac{\exp(\mathrm{i}\xi y_0)}{\gamma^-(k_1, \xi, \omega)}\left[\frac{1}{(\xi - k_2)(\xi - 2\mathrm{i}/a)(\xi + 2\mathrm{i}/a)}\right]\mathrm{d}\xi, \tag{D 1}$$

with the integration contour lying along the real axis, indented above the pole at $\xi = k_2$. The first step is to resolve the term in square brackets in the integrand of (D 1) into partial fractions, so that I_2 can be expressed as a sum of three integrals, i.e.

$$I_2 = \frac{1}{1 + \frac{1}{4}k_2^2a^2}\int\frac{\exp(\mathrm{i}\xi y_0)}{\gamma^-(k_1, \xi, \omega)(\xi - k_2)}\mathrm{d}\xi - \frac{1}{\mathrm{i}ak_2 + 2}\int\frac{\exp(\mathrm{i}\xi y_0)}{\gamma^-(k_1, \xi, \omega)(\xi - 2\mathrm{i}/a)}\mathrm{d}\xi$$
$$+ \frac{1}{\mathrm{i}ak_2 - 2}\int\frac{\exp(\mathrm{i}\xi y_0)}{\gamma^-(k_1, \xi, \omega)(\xi + 2\mathrm{i}/a)}\mathrm{d}\xi. \tag{D 2}$$

In each of the three integrals in (D 2) the integration contour is now deformed from the real axis onto the contour wrapped round the branch line in the upper half of the ξ-plane; we note that in doing this a pole contribution to the second integral is picked

up from the pole at $\xi = 2\mathrm{i}/a$. The three branch-line integrals can now be completed in exactly the same way as was described in Appendix A for I_1, and adding these three expressions to the pole contribution we find finally that

$$I_2 = -2\pi\mathrm{i}\frac{\exp(\mathrm{i}k_2 y_0)\{1-\mathrm{erf}[\exp(\frac{1}{4}\mathrm{i}\pi)\, y_0^{\frac{1}{2}}\gamma^-(k_1,k_2,\omega)]\}}{\gamma^-(k_1,k_2,\omega)(1+\frac{1}{4}k_2^2a^2)}$$

$$-2\pi\mathrm{i}\frac{\exp(-2y_0/a)\,\mathrm{erf}[\exp(\frac{1}{4}\mathrm{i}\pi)\, y_0^{\frac{1}{2}}\gamma^-(k_1,2\mathrm{i}/a,\omega)]}{(\mathrm{i}ak_2+2)\gamma^-(k_1,2\mathrm{i}/a,\omega)}$$

$$-2\pi\mathrm{i}\frac{\exp(2y_0/a)\{1-\mathrm{erf}[\exp(\frac{1}{4}\mathrm{i}\pi)\, y_0^{\frac{1}{2}}\gamma^-(k_1,-2\mathrm{i}/a,\omega)]\}}{(\mathrm{i}ak_2-2)\gamma^-(k_1,-2\mathrm{i}/a,\omega)}. \qquad \text{(D 3)}$$

REFERENCES

Abramowitz, M. & Stegun, I. A. 1968 *Handbook of Mathematical Functions*. Dover.

Amiet, R. K. 1976 High frequency thin-airfoil theory for subsonic flow. *AIAA J.* **14**, 1076–1082.

Amiet, R. K. 1986*a* Airfoil gust response and the sound produced by airfoil–vortex interaction. *J. Sound Vib.* **107**, 487–506.

Amiet, R. K. 1986*b* Intersection of a jet by an infinite span airfoil. *J. Sound Vib.* **111**, 499–503.

Dowling, A. P. & Ffowcs Williams, J. E. 1983 *Sound and Sources of Sound*. Ellis Horwood.

Ffowcs Williams, J. E. & Guo, Y. P. 1988 Sound generated from the interruption of a steady flow by a supersonically moving aerofoil. *J. Fluid Mech.* **195**, 113–135.

Guo, Y. P. 1990 Sound generation by a supersonic aerofoil cutting through a steady jet flow. *J. Fluid Mech.* **216**, 193–212.

Howe, M. 1989 On sound generated when a vortex is chopped by a circular airfoil. *J. Sound Vib.* **128**, 487–503.

Jones, D. S. 1966 *Generalised Functions*. McGraw-Hill.

Koiter, W. T. 1954 Approximate solution of Wiener–Hopf type integral equations with applications, I–III. *Koninkl. Ned. Akad. Wetenschap. Proc.* B**57**, 558–579.

Martinez, R. & Widnall, S. E. 1983 Aerodynamic theory for wing with side edge passing subsonically through a gust. *AIAA J.* **21**, 808–815.

Miles, J. W. 1951 The oscillating rectangular airfoil at supersonic speeds. *Q. Appl. Maths* **9**, 47–65.

Noble, B. 1958 *Methods Based on the Wiener–Hopf Technique*. Pergamon.

Peake, N. 1992 Unsteady transonic flow past a quarter-plane. *J. Fluid Mech.* **244**, 377–404.

Simonich, J. C., McCormick, D. C. & Lavich, P. L. 1989 Interaction noise mechanisms for advanced propellers: experimental results. *AIAA Paper* 89-1093.

Stewartson, K. 1950 On the linearized potential theory of unsteady supersonic motion. *Q. J. Mech. Appl. Maths* **3**, 182–199.

Vaczy, C. M. & McCormick, D. C. 1987 A study of the leading edge vortex and tip vortex on prop-fan blades. *J. Turbomachinery* **109**, 325–331.